J. Schreiber, B. Salbert, C.L. Bottasso
Study of Wind Farm Control Potential Based on SCADA Data
Journal of Physics: Conference Series, Vol. 1037, N. 3, 2018, 032012 (13 pages)
doi:10.1088/1742-6596/1037/3/032012

Study of wind farm control potential based on SCADA data

IOP Conf. Series: Journal of Physics: Conf. Series **1037** (2018) 032012 doi:10.1088/1742-6596/1037/3/032012

Study of wind farm control potential based on SCADA data

J Schreiber[1], B Salbert[1], C L Bottasso[1,2]

[1] Wind Energy Institute, Technische Universität München, Boltzmannstraße 15, D-85748 Garching bei München, Germany

[2] Dipartimento di Scienze e Tecnologie Aerospaziali, Politecnico di Milano, Via La Masa 34, I-20156 Milano, Italy

E-mail: {johannes.schreiber, bastian.salbert, carlo.bottasso}@tum.de

Abstract. In this work, a control-oriented wind farm model is validated against SCADA data from a typical on-shore wind farm, without additional instrumentation available. The comparison of model-predicted and measured power deficits due to wake impingement shows good agreement. Furthermore, the model is used to compute optimum yaw misalignments for yaw-induced wake steering, leading to an estimated 1.7 % increase in annual energy production by mitigation of wake losses. Results show that wake steering based on standard SCADA data, which is usually available in operational wind farms, has promising potential for open-loop model-based wind farm control.

1. Introduction

Wake interactions within wind farms lead to power losses and increased fatigue loading. Wind farm control (WFC) aims at mitigating these wake effects by operating the turbines within a plant in a coordinated manner. This is in contrast with the current greedy policy, where each machine operates individually to maximize its own power capture [1]. Recent approaches focus on increasing plant-level power capture by axial induction or wake redirection control [2, 3]. The latter seems to be a particularly promising approach, and it works by laterally steering wakes through the intentional misalignment of the rotor with respect to the incoming wind vector.

For a computationally efficient prediction of wake behavior and turbine power production, parametric wind farm models have been developed, facilitating WFC design and application [4]. This study validates such a model for baseline operation, and then uses it to investigate the potential increase in annual energy production (AEP) by yaw-induced wake steering.

In a first step, results from the well-known FLORIS (FLOw Redirection and Induction in Steady-state) [5] wake model are compared to historical 10 minute SCADA (Supervisory Control and Data Acquisition) measurements from a typical on-shore wind farm. Ambient wind direction is estimated from calibrated turbine yaw measurements, and undisturbed inflow is established from free-stream reference turbines. The model is able to predict power losses due to wake interactions with good accuracy for all investigated wind directions. In fact, the simulated AEP matches measurements within a 1.4 % accuracy.

Finally, the potential increase in AEP is estimated using a model-based wake steering strategy, termed here "advanced sector management". Thereby, pre-calculated optimum yaw

misalignments are set for the individual turbines as a function of ambient wind conditions. For the investigated cluster of wind turbines, a potential increase in AEP of 1.7 % is obtained.

2. Models, methods and power plant

2.1. Wind farm model

The FLORIS wake model [5] together with the Jiménez deflection model [6] are employed within a wind farm framework, which is able to account for arbitrary plant setups with irregular turbine positions, differing hub heights and machine types. The combined velocity reduction of overlapping wakes is derived from the superposition of the energy deficits in the individual wakes, according to the Katic [7] wake interaction model. It was verified that the model implementation gives results identical to the public-domain TU Delft code [8].

The parameter set from Gebraad et al. [4], reported in table 1, is used for all turbines. These parameter values were used "as is", without any further tuning for the specific site considered here.

Table 1: FLORIS parameters for the NREL 5MW turbine, identified from CFD simulations in a neutral atmospheric boundary layer with $TI = 6\,\%$ by Gebraad et al. [4]

Power		Wake					
		Deflection		Expansion		Velocity	
p_P	1.88	k_d	0.15	k_e	0.065	$M_{\mathrm{U},1}$	0.5
		a_d	−4.5	$m_{\mathrm{e},1}$	−0.5	$M_{\mathrm{U},2}$	1
		b_d	−0.01	$m_{\mathrm{e},2}$	0.22	$M_{\mathrm{U},3}$	5.5
				$m_{\mathrm{e},3}$	1	a_U	5
						b_U	1.66

Wind-speed-dependent turbine power and thrust coefficients derived from publicly available power curves are assigned to each turbine in the wind farm. Power down-rating for noise reduction at night can be considered by altering the performance curves accordingly. During simulation, thrust and power coefficients are interpolated [9] and power is calculated for each turbine as function of rotor-averaged wind speed.

Besides the wind farm setup and wake model parametrization, the model inputs are represented by ambient wind speed, direction, shear and air density. A change in ambient turbulence intensity could be considered by adapting the wake expansion parameter for the whole power plant.

2.2. Test wind farm

Windpark Dornum is located in north-western Germany, 5 km away from the North Sea. It is surrounded by flat grassland except for two small villages east- and north-westwards of the wind farm, approximately 1 km away. The region is very populated with wind turbines, ranging from small ~ 100 kW to large multi-MW machines that are owned and operated by different parties. Figure 1 gives a view of the southward wind farm section.

SCADA data of 12 wind turbines was provided by the operator and used for the present study. While this complete set is used for the WFC potential analysis, only a cluster of six identical turbines (E-70, rotor diameter 71 m, hub height 64 m) is utilized for model validation, enabling a direct analysis of wake-caused power deficits, as explained later on more in detail. As shown in figure 2, the investigated turbines are in proximity of several machines of different sizes. Only the wakes of the closest 45 turbines are taken into account in this study, while more than 100 additional turbines further away are not considered, as their influence is expected to be small.

Figure 1: Photograph of Windpark Dornum, taken from PD210 looking towards the south.

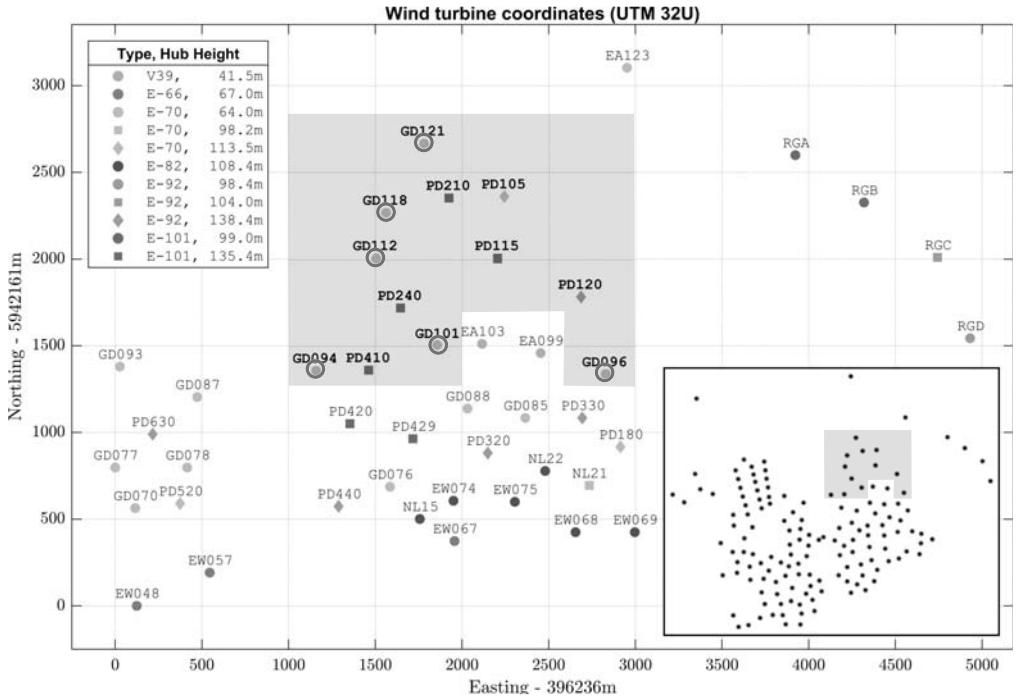

Figure 2: Arrangement of the 45 simulated wind turbines. The grey rectangle encloses the 12 measurement turbines used for optimization; red circles highlight the six E-70 turbines with 64 m hub height used for validation. The subplot in the lower right corner shows all surrounding turbines, including the ones not used in the simulation.

A full year of 10 minute averaged SCADA measurements was provided, from which the nacelle anemometer wind speed, measured turbine power (and its extreme values) and yaw orientation are employed. Therefore, the complete data set comprises 52 704 data points for each of the 12 turbines.

The raw data is prepared using a three-step procedure: firstly, data is pre-processed and formatted (conversion of time stamps to UTC+1, removal of duplicate measurements, etc.). Secondly, turbine measurements are discarded in case of

turbine malfunction: turbine status indicating a malfunction,

no power production: power smaller than 5 kW or rotor speed smaller than 1 rpm, or
outliers: anomalous conditions, detected by comparing the anemometer wind speed with power measurements. In case of wind speed above rated and a power production deviating more than 5 % from nominal (or night-reduced) rated power, the condition is marked as an outlier. These conditions are believed to mainly originate from unscheduled power curtailments demanded by the grid operator.

The resulting number of discarded data points for the individual turbines is summarized in table 2. Note that one data point can belong to multiple categories at once.

Finally, the remaining data is aggregated into a set of data points, valid for all individual turbines simultaneously. Overall, the data preparation leaves 33 635 ($\approx$ 64 %) of "good" data points for further usage.

2.3. Determination of ambient wind conditions

In the absence of additional measuring devices such as meteorological masts or LIDARs, the ambient wind conditions must be estimated from SCADA data alone. A method has been developed that first estimates the ambient wind direction from turbine yaw measurements, and then identifies a set of undisturbed free-stream turbines. In turn, these are used for calculating ambient wind speed, turbulence and vertical wind shear.

The ambient wind direction can be obtained from the average yaw orientation of all turbines, rather than using wind vane measurements. In fact, on-board wind vane measurements are often not recorded by the SCADA system, which is also the case for the wind farm under consideration. In addition, wind vanes might not always be very accurate, due to their point-wise nature and disturbances from blade passage, rotor wake and nacelle interference effects. Given that the yaw position sensors are usually poorly calibrated (typically, only for rewinding purposes), the average 12-turbine yaw angle is manually corrected by a constant scalar offset to fit the observed power deficit positions to the waking wind directions expected from the wind farm layout. A similar procedure was used by [10, 11, 12], using the yaw signal of only one single reference turbine. In this work, the approach is extended by using the average pointing direction of the entire wind farm. Using multiple yaw signals increases the confidence in the determined ambient wind direction and compensates for turbulent wind direction fluctuations over the area of the wind farm. For larger clusters of wind turbines, more sophisticated models could be employed to also account for large-scale variations of wind direction.

Free-stream turbines are used to determine ambient wind speed, turbulence, shear and reference power, as described later on. The determination of whether a turbine operates in free-stream or not, is here obtained by evaluating the wind farm model with a conservative wake expansion coefficient. A turbine is defined as operating in free-stream if, for a certain wind direction, it does not experience power losses from wake impingement. In the present study, the wakes of all 45 simulated wind turbines are taken into account for the determination of free-stream conditions. The free-stream turbines identified in this way (out of the set of six E-70 turbines) are shown in figure 3 for varying wind directions.

To measure ambient wind speed, it is generally advantageous to use the rotor effective wind speed (REWS) instead of the point-wise measurements provided by the nacelle anemometer. Even though the latter might be partially corrected for turbine induction as well as nacelle and blade induced flow disturbances, the REWS is a better indicator for overall ambient wind speed. There are different methods for REWS estimation discussed in the literature [13, 14]. Most of these methods usually require detailed turbine information, which is however often not available. Therefore, this work estimates REWS simply by using publicly available curves of turbine power versus wind speed. Thereby, given the SCADA measured power, the wind speed is readily obtained from the power curve of the corresponding turbine. Note that, by using such technique, a non-ambiguous REWS determination is only possible between cut-in and rated

Table 2: Number of data points discarded for each turbine.

Turbine ID	Turbine Malfunction	No Power Production	Outliers
GD094	249	5506	394
GD096	850	6337	353
GD101	847	8032	651
GD112	993	8136	651
GD118	898	9208	715
GD121	921	7877	616
PD105	94	5764	723
PD115	272	5628	1384
PD120	280	5290	706
PD210	894	8573	1732
PD240	147	5944	1533
PD410	130	5877	1321

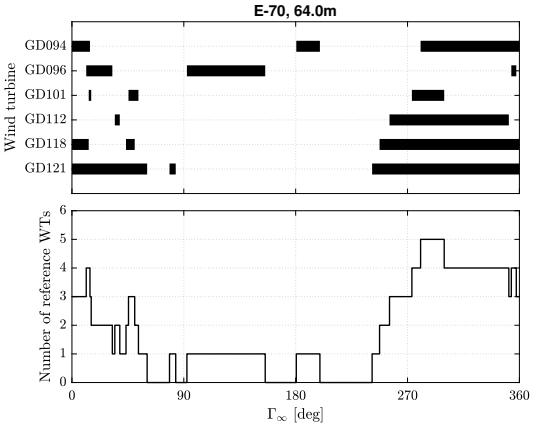

Figure 3: Free-stream reference turbines as functions of wind direction by name (top) and resulting number (bottom).

power (control region II, or partial load). In this work, the ambient wind speed is obtained by averaging the REWS of all free-stream turbines. In case that no free-stream turbine exists or can provide a REWS estimate, the ambient wind speed cannot be determined and the data point has to be removed (see next section). As for the ambient wind direction, more sophisticated averaging methods could be used in larger power plants to account for a variation of ambient wind speed throughout the farm.

Note that REWS obtained from power curve lookup is inherently normalized by the constant reference air density of the power curve. If such REWS is used as ambient wind speed in the model simulations, it matches simulated to measured free-stream power exactly, provided that the same constant reference density $\rho_{\mathrm{ref}} = 1.225\,\mathrm{kg/m^3}$ and power curves are used. Remaining power deviations occur only on waked turbines and are caused by inaccurate predictions of the wake model.

A measure for ambient turbulence is derived from turbine power fluctuations in control region II, similarly to the method proposed by Mittelmeier et al. [12]. In the present case, no 10 min power standard deviation is available in the SCADA data, so that the 10 min extreme values P_{min} and P_{max} are used to define the turbulence measure TI_{P}:

$$TI_{\mathrm{P}} := \frac{P_{\mathrm{max}} - P_{\mathrm{min}}}{P}. \tag{1}$$

The data set was split in two equal parts, according to measurements recorded below or above the median turbulence intensity, herein called *low TI* and *high TI*, respectively.

In case of a wind farm with turbines of different hub height, it is also possible to estimate the vertical wind shear profile. In fact, using simultaneously the free-stream turbine anemometer wind speed measurements at two or more different hub heights, the average power law exponent [15] can be identified. In this work, SCADA measurements of turbines with 64 m and 135.4 m hub height are available, and therefore a yearly average power law exponent of $\alpha \approx 0.3$ could be identified by choosing 64 m as the reference height. This value is used in all model simulations.

3. Results

3.1. Validation

The main purpose of the wind farm flow model is to correctly predict power losses due to wake impingement on downstream turbines. Such wake losses are evaluated with respect to the power

available in the undisturbed inflow, which is here determined from the free-stream turbines. At least one such reference turbine must be available for a given wind direction to enable the determination of power deficits.

To utilize the determined reference power directly —without the need of correcting for turbine type and wind shear (hub height)—, only the set of six identical E-70 turbines with a 64 m hub height is used for validation. For this cluster, due to the large number of surrounding turbines, no free-stream reference turbines are available for 38 % of the data points in the cleaned data set.

Furthermore, measured ambient wind speed and direction must be available to feed the wind farm model. The method presented in section 2.3 does not allow one to infer REWS in control region III (full power). Therefore, the validation has to be limited to conditions in which at least one reference turbine operates below rated wind speed, discarding an additional 0.5 % of the cleaned data points.

The model is simulated for time series of measured ambient wind speed and direction with a constant shear and air density. To increase computational efficiency, the power of all wind turbines is pre-calculated on a grid of discrete wind speeds $V_\infty = [1, 2, \ldots, 25\,\mathrm{m\,s^{-1}}]$ and directions $\Gamma_\infty = [0, 5, \ldots, 355°]$. This grid is then used to extract time series of simulated power as function of measured wind speed and direction via linear interpolation.

Time series of both simulated and measured normalized power are then binned over wind directions, thereby inherently considering the statistical distribution of the data points. The power ratio assigned to each 5°-wide wind direction bin is calculated via the median, as this is more robust against outliers in the scattered data. To base the validation on as many data points as possible —and thereby increase the confidence in the results—, no additional restrictions are imposed on the evaluated range of wind speeds.

In figure 4, the measured power over wind direction is shown, both point-wise as well as by the binwise median for each of the six turbines. The latter case is calculated from low and high-turbulent measurements separately, and it is shown by the blue and red solid lines, respectively. The black solid line illustrates the corresponding simulation results, also generated by binning time series of power ratio into 5°-wide wind direction bins. Errorbars visualize the binwise standard deviation of simulated power deficits caused by the described wind speed dependency. Different turbulence levels are not considered in the simulations, as only one fixed set of parameters is used. In the figure, a histogram represents the total time of available measurements for each wind direction bin and turbulence group.

The results show a good overall agreement between model-predicted and measured normalized power. However, for southern and western wind directions, simulated P/P_ref tends to be too large, as can be observed very distinctly for GD094 and also by looking at the wind farm efficiency in figure 5. This effect likely originates from upwind turbines that are not considered in the simulation (cf. figure 2), but whose influence is seen in the measurements. Furthermore, non-physical peaks $P/P_\mathrm{ref} > 1$ can be noticed in the measurements, for example for GD121 over the entire range of wind directions. In those cases the reference power P_ref used for normalization is smaller than the turbine power P, possibly due to noise in the measurements or unmodeled flow effects in the determination of the reference turbines. Generally speaking, normalized power can be affected by inaccurate estimates of reference power, which could in fact be another source for the mentioned deviations with southern and western winds. At these wind directions, low confidence can be placed on the reference power that is determined from only one single free-stream turbine.

The measured low-turbulent power deficits tend to be deeper and narrower due to reduced wake mixing and lower wind direction uncertainty [16]. These effects of turbulence on apparent wake expansion and decay could potentially be modeled by adapting the FLORIS wake expansion parameter k_e. The simulation results correlate slightly better to the low-turbulence

measurements, which is in accordance with the fact that wake parameters were originally identified for low ambient turbulence. Further improvements are to be expected if the model parameters are calibrated explicitly for the specific site and turbines.

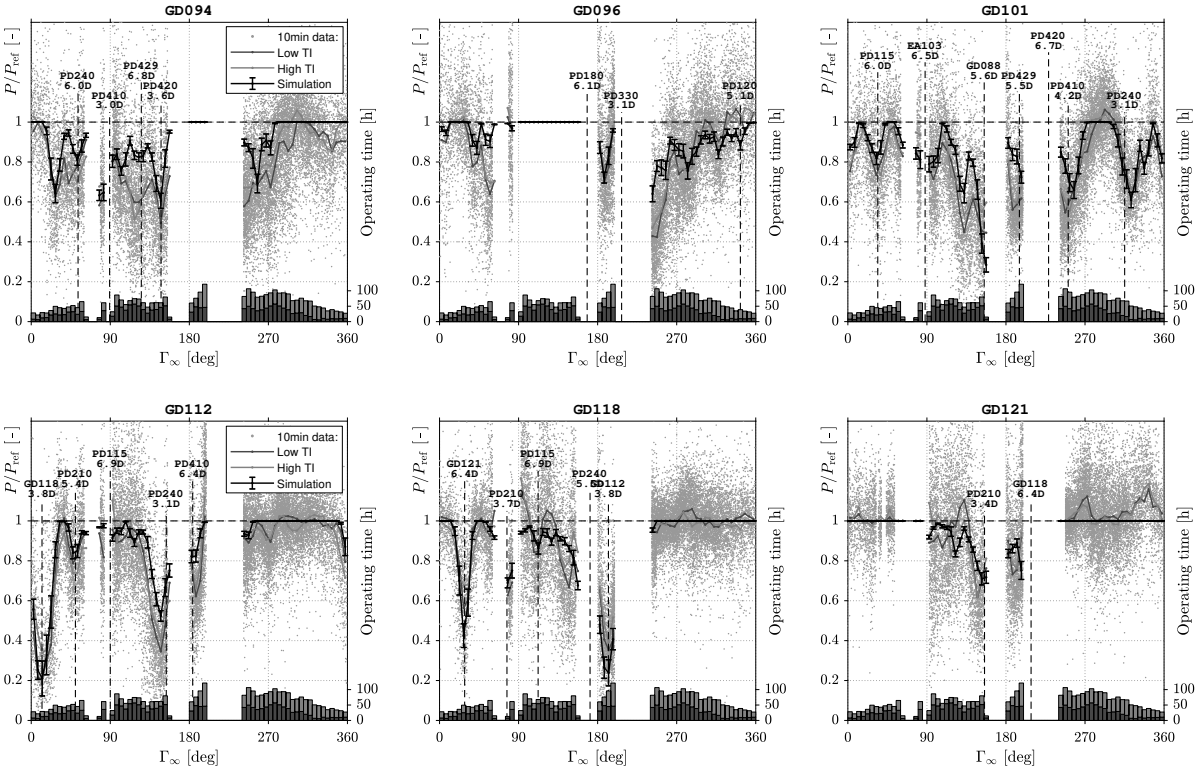

Figure 4: Simulated and measured E-70 power ratio for the year 2016. The 10 min SCADA measurements are given both directly and by their binwise median, which is split according to TI_{P}. The simulations are given by their binwise medians, vertical bars illustrating the standard deviation due to wind speed dependency within each bin. Vertical lines indicate waking turbines for normalized distances $< 7\,\mathrm{D}$. The histogram represents the total time of available measurements for each wind direction bin and turbulence group.

As for the individual turbines, the combined power ratio of the six turbines is evaluated in figure 5 in terms of wind farm efficiency η_{WF}, defined as

$$\eta_{\mathrm{WF}} = \frac{\sum_{i=1}^{N_{\mathrm{T}}} P_i}{N_{\mathrm{T}} P_{\mathrm{ref}}}, \tag{2}$$

where P_i is the power of wind turbine i, P_{ref} is the free-stream reference power, and N_{T} is the total number of considered wind turbines. As for the individual turbines, the simulated wake losses correspond well with the measurements.

By integrating time series of power over time, the measured and simulated AEP can be computed for the considered turbines, as summarized in table 3. The six turbines together lose circa 11 % of the energy available in the ambient inflow due to wake interactions. The wind farm model predicts the actual wind farm AEP with 1.38 % accuracy, although deviations of almost 7 % occur for the individual machines.

Note that the parameters k_{d}, related to the wake deflection, and p_{P}, describing power reduction in yawed operation, could not be validated using the available set of measurements.

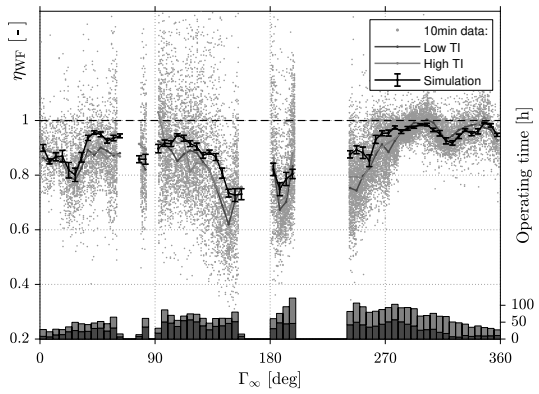

Figure 5: Combined efficiency of the six E-70s, in analogy to figure 4.

Table 3: Measured and simulated wind turbine AEP [GWh].

Turbine ID	AEP meas,ref	AEP meas	AEP sim	Error [%]
GD094	1.27	1.07	1.15	+6.72
GD096	1.27	1.11	1.14	+2.56
GD101	1.27	1.03	1.09	+6.37
GD112	1.27	1.15	1.17	+1.51
GD118	1.27	1.17	1.12	−3.83
GD121	1.27	1.25	1.20	−3.62
Wind farm	7.64	6.77	6.87	+1.38

3.2. Analysis of wake steering potential

Next, the wind farm model is used to estimate the potential increase in power and AEP by wake steering. Therefore, the yaw angles $\vec{\gamma} = (\gamma_1, \gamma_2, \ldots, \gamma_{N_\mathrm{T}})$ of the $N_\mathrm{T} = 12$ considered turbines are optimized to maximize total wind farm power, by solving the following problem:

$$\max_{\vec{\gamma}} \sum_{i=1}^{N_\mathrm{T}} P_i(V_\infty, \Gamma_\infty, \vec{\gamma}). \tag{3}$$

The yaw misalignments $\Delta\gamma_i = \gamma_i - \Gamma_\infty$ with respect to the wind direction Γ_∞ are constrained to $\pm 30°$ as in [9].

The optimization problem is solved using the `Matlab` global-optimization patternsearch solver [17]. In contrast to gradient-based optimization algorithms, this direct-search solver can handle the discontinuities in calculated wind farm power originating from the discrete wake velocity profiles.

For an exemplary turbine (GD118) of the wind farm under consideration, figure 6 shows the computed optimum yaw misalignments obtained for discrete combinations of ambient wind directions Γ_∞ and speeds V_∞. Such look-up tables could be used to control the wind farm in open-loop, providing optimum turbine misalignments based on the ambient wind speed and direction identified from free-stream turbines. Figure 7 shows the relative wind farm power gains $\Delta P/P_\mathrm{baseline}$ corresponding to the optimum yaw misalignments.

The results show that, as expected and according to intuition, wake steering is most effective for wind directions with several aligned turbines and for wind speeds in region II of the power curve. In fact, no losses can be mitigated and no power gains are possible if no wake losses occur in the first place. This can be either because no wake interactions take place for certain wind directions, or because wake interactions do not have an effect when the wind speed is sufficiently high for all turbines to operate at rated power. The latter phenomenon occurs towards the typical rated wind speed $V \approx 12\,\mathrm{m\,s^{-1}}$, when upwind turbines limited to rated power leave more and more power in the flow for downwind machines. The power gains achievable by wake steering diminish, and so do the proposed optimum upwind turbine misalignments. This wind speed dependency emerges solely from the underlying turbine performance curves, and it is not a threshold imposed by the authors. Figure 7 shows that the largest power gain $\Delta P/P_\mathrm{baseline} = 1.2\,\mathrm{MW}/7\,\mathrm{MW} \approx 17\,\%$ occurs at $\Gamma_\infty = 205°$ and $V_\infty = 4\,\mathrm{m\,s^{-1}}$. The flow field around the 12 optimized turbines before and after optimization is shown in figure 8 for $\Gamma_\infty = 205°$ and $V_\infty = 8\,\mathrm{m\,s^{-1}}$. The figure clearly illustrates how wakes are steered away from downwind turbines.

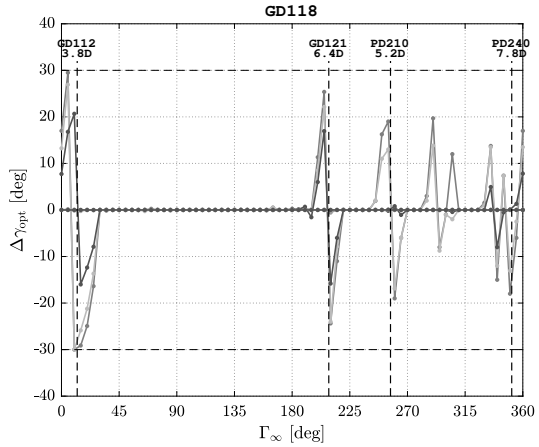

Figure 6: Optimum yaw misalignments $\Delta\gamma_{\mathrm{opt}}$ for an exemplary turbine (GD118) as functions of ambient wind direction Γ_∞ and speed V_∞. Relative directions and distances ($< 9\,\mathrm{D}$) of power-maximized downwind turbines are displayed.

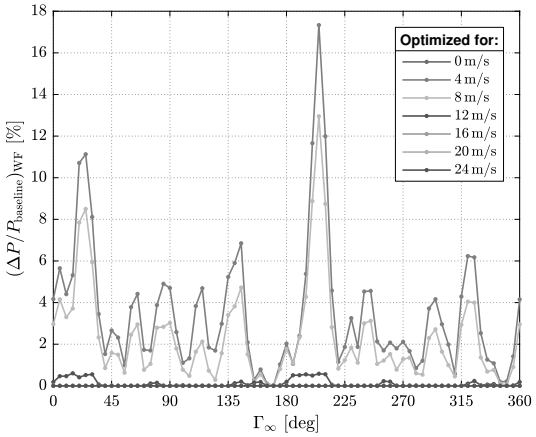

Figure 7: Relative power gain for the 12 measurement turbines as function of ambient wind direction Γ_∞ and speed V_∞.

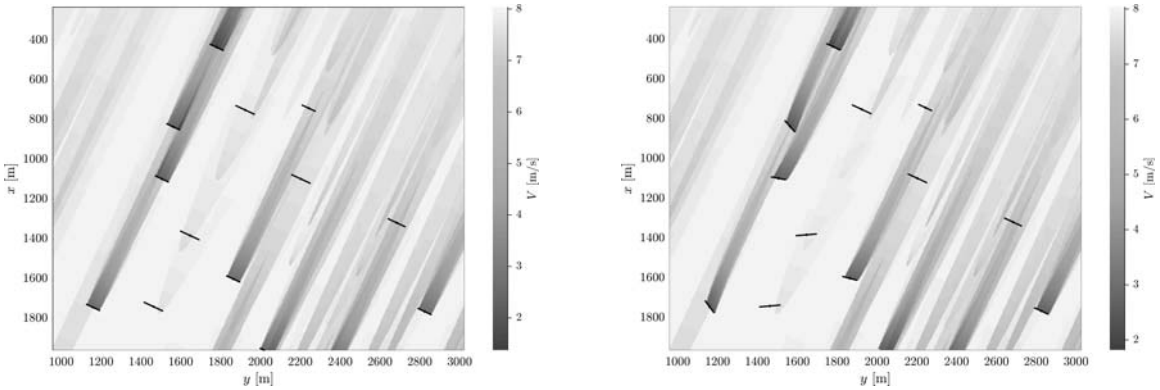

Figure 8: Velocity field around the 12 optimized turbines, before (left) and after (right) optimization for $\Gamma_\infty = 205°$ and $V_\infty = 8\,\mathrm{m/s}$, visualized on a horizontal plane at $z = 64\,\mathrm{m}$. The wakes of some turbines of different hub height are only partially visible. Wakes of surrounding turbines are also visible.

To determine the potential increase in wind farm AEP using the proposed look-up table for advanced sector management, the distributions of ambient wind speed and direction at the given site should be known. As shown in the previous section, for several wind directions all evaluated turbines are waked by upstream turbines for which no data is available. To avoid loosing too many measurement points, it was decided to ignore wake effects and compute the yearly wind speed distribution based on all six E-70 nacelle anemometer measurements. Clearly, the average wind speed and therefore the absolute AEP will be underestimated, but the relative increase in AEP should not be significantly affected. The ambient wind direction is obtained as discussed in section 2.3. The resulting wind speed distribution and wind rose are shown in figure 9.

The wind farm efficiency can be determined as a function of wind direction, by evaluating the wind farm model for the identified ambient wind conditions without (baseline) and with (optimized) wake steering, as shown in figure 10. Even though the wind farm efficiency increases over the entire range of wind directions, it is important to note that the surrounding 33 turbines are not optimized. Larger improvements are to be expected by including them into

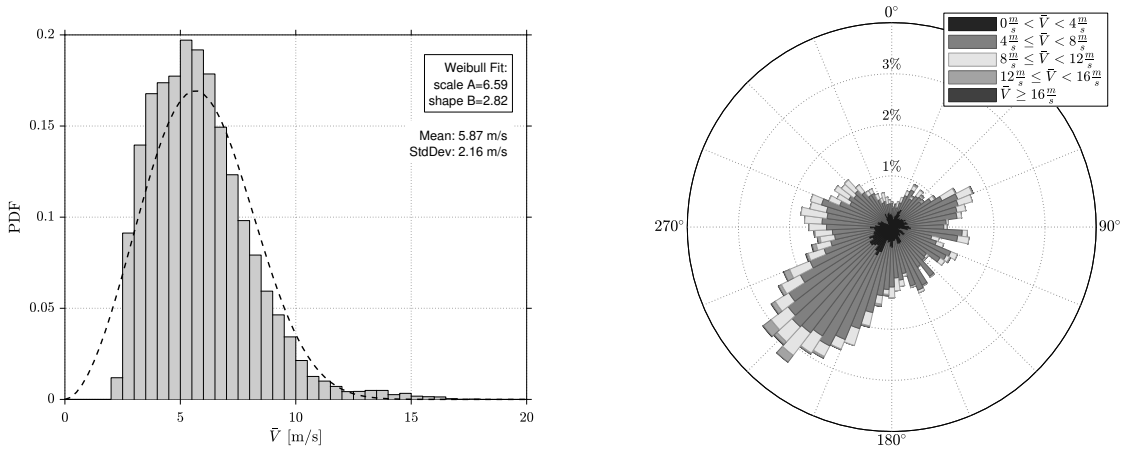

Figure 9: Measured and Weibull-fitted wind speed distribution (left) and wind rose (right) for the year 2016.

the optimization.

Accumulating over all measurements, an AEP increase

$$\Delta AEP/AEP_{\text{baseline}} = 0.64\,\text{GWh}/38.03\,\text{GWh} \approx 1.7\,\%$$

is predicted by the wind farm model when wake steering is implemented on the cluster of 12 turbines.

If the yaw angles are only optimized for the constant site average wind speed, the resulting look-up table is only a function of wind direction and therefore possibly simpler to implement. In such case, the estimated AEP gain decreases to 1.3 %. This is less than the stated 1.7 % achieved with a wind speed and direction dependent look-up table, as power curve effects are not considered.

The underlying distribution of yaw misalignments shown in figure 11 reveals that, statistically, the majority of the proposed optimum misalignments is rather small, as also observed in [18]. In the present case, almost 80 % of the misalignments are smaller than 5° and the misalignment threshold is rarely reached. Therefore, limiting the maximum allowed misalignment angles to the above stated ±30° will only have a small influence on the AEP gain as demonstrated by [18], but might increase turbine lifetime by limiting turbine loading [19]. The given distribution of yaw misalignments could be used to trade off the costs associated with wake steering against the energy gains, to ultimately minimize the cost of energy. Employing damage models [20] and performing such an analysis could be the subject of further research beyond the scope of the present work.

4. Conclusions and outlook

This work presented the application of the FLORIS wake model to an operational on-shore wind farm, with two main goals: validating model predictions against SCADA measurements, and estimating the potential of wake steering for a given set of turbines.

Firstly, it was shown that ambient wind direction and free-stream flow properties can be estimated solely from turbine SCADA data, without additional instrumentation.

Secondly, statistical comparisons have shown that the model-predicted wind turbine power deficits and wind farm efficiency are in good agreement with field measurements.

Finally, the wind farm model was employed to find optimum turbine yaw misalignments that maximize wind farm power by yaw-induced wake steering. For each turbine, a look-up table of optimum yaw misalignment as a function of wind direction and speed is obtained that could be

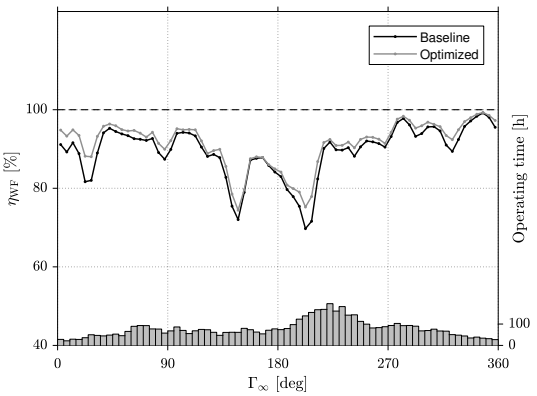

Figure 10: Simulated baseline and optimized wind farm efficiency at measured wind direction and speed. Additionally, the distribution of measured wind directions (operating time) is displayed at the bottom of the plot.

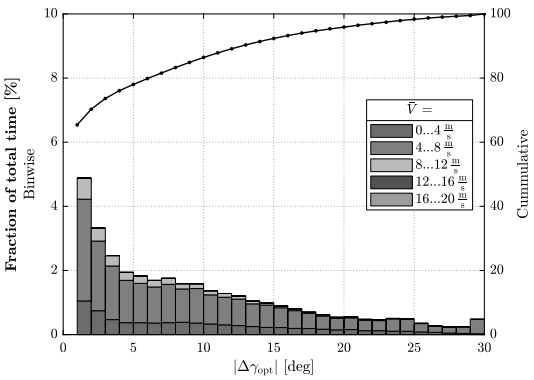

Figure 11: Distribution of the optimum yaw misalignments, shown for $|\Delta\gamma_{\text{opt}}| > 1°$.

used to implement open-loop wake steering in the field. For the studied cluster of 12 turbines, a maximum power gain of 17 % is predicted for southward wind directions at low wind speeds. Based on one year of site-specific wind conditions, a 1.7 % AEP gain can be expected. The necessary yaw misalignments were limited to ±30°, about 80 % of them being smaller than 5°.

Acknowledgments

The authors thankfully acknowledge Mr. Rik Folkerts and Mr. Thomas Erdmann of Windpark Dornum GmbH for providing measurement data and valuable support. This work has been partially supported by the CL-Windcon project, which receives funding from the European Union Horizon 2020 research and innovation programme under grant agreement No. 727477.

References

[1] Knudsen T, Bak T and Svenstrup M 2015 *Wind Energy* **18** 1333–1351 ISSN 10954244
[2] Boersma S, Doekemeijer B M, Gebraad P, Fleming P A, Annoni J, Scholbrock A K, Frederik J A and van Wingerden J W 2017 A tutorial on control-oriented modeling and control of wind farms *American Control Conference 2017* (IEEE) p 1–18 ISBN 978-1-5090-5992-8
[3] Fleming P, Annoni J, Shah J J, Wang L, Ananthan S, Zhang Z, Hutchings K, Wang P, Chen W and Chen L 2017 *Wind Energy Science* **2**(1) 229–239 ISSN 2366-7451
[4] Gebraad P M O, Teeuwisse F W, Van Wingerden J W, Fleming P A, Ruben S D, Marden J R and Pao L Y 2016 *Wind Energy* **19** 95–114 ISSN 10954244
[5] Gebraad P M O, Teeuwisse F W, Van Wingerden J W, Fleming P A, Ruben S D, Marden J R and Pao L Y 2014 A data-driven model for wind plant power optimization by yaw control *American Control Conference (ACC), 2014* (Piscataway, NJ: IEEE) pp 3128–3134 ISBN 978-1-4799-3274-0
[6] Jiménez A, Crespo A and Migoya E 2010 *Wind Energy* **13** 559–572 ISSN 10954244
[7] Katic I, Højstrup J and Jensen N O 1986 A simple model for cluster efficiency *European Wind Energy Association Conference and Exhibition* p 407–410
[8] Storm R and Doekemeijer B An exhaustive matlab implementation of the steady-state floris wind farm model URL `https://github.com/TUDelft-DataDrivenControl/FLORISSE_M`
[9] Gebraad P, Thomas J J, Ning A, Fleming P and Dykes K 2017 *Wind Energy* **20**(1) 97–107 ISSN 10954244
[10] Hansen K S, Barthelmie R J, Jensen L E and Sommer A 2012 *Wind Energy* **15**(1) 183–196 ISSN 10954244
[11] Infield D and Zorzi G 2017 *Journal of Physics: Conference Series* **854** 012024 ISSN 1742-6588
[12] Mittelmeier N, Allin J, Blodau T, Trabucchi D, Steinfeld G, Rott A and Kühn M 2017 *Wind Energy Science Discussions* 1–20 ISSN 2366-7621
[13] Bottasso C L, Cacciola S and Schreiber J 2018 *Renewable Energy* **116** 155–168
[14] Soltani M N, Knudsen T, Svenstrup M, Wisniewski R, Brath P, Ortega R and Johnson K 2013 *IEEE Transactions on Control Systems Technology* **21**(4) 1155–1167 ISSN 1063-6536

[15] James F Manwell J G M and Rogers A L 2009 *Wind energy explained* (Wiley) ISBN 978-0-470-01500-1
[16] Gaumond M, Réthoré P E, Ott S, Peña A, Bechmann A and Hansen K S 2014 *Wind Energy* **17**(8) 1169–1178 ISSN 10954244
[17] patternsearch: Find minimum of function using pattern search URL `https://de.mathworks.com/help/gads/patternsearch.html`
[18] Fleming P A, Ning A, Gebraad P M O and Dykes K 2016 *Wind Energy* **19**(2) 329–344 ISSN 10954244
[19] Fleming P, Gebraad P M, Lee S, van Wingerden J W, Johnson K, Churchfield M, Michalakes J, Spalart P and Moriarty P 2015 *Wind Energy* **18**(12) 2135–2143 ISSN 10954244
[20] Damiani R, Dana S, Annoni J, Fleming P, Roadman J, van Dam J and Dykes K 2017 *Wind Energy Science Discussions* 1–25 ISSN 2366-7621